

Diet-Induced Obesity and Insulin Resistance are Associated with Brown Fat Degeneration in SIRT1-Deficient Mice

Fen Xu^{1,2*}, Xiaobin Zheng^{1,2*}, Beisi Lin^{1,2}, Hua Liang^{1,2}, Mengyin Cai^{1,2}, Huanyi Cao^{1,2}, Jianping Ye³, and Jianping Weng^{1,2}

Objective: Recent studies have revealed that SIRT1 gain-of-function could promote adipose tissue browning for the adaptive thermogenesis under normal diet. This study investigated the role of SIRT1 loss-of-function in diet-induced obesity and insulin resistance and the mechanism involved in adipose tissue thermogenesis.

Methods: Male *SIRT1*^{+/-} and wild-type (WT) mice were fed with a high-fat diet (HFD) for 16 weeks to induce obesity and insulin resistance, while mice on a chow diet were used as lean controls. The phenotype data were collected, and different adipose tissue depots were used for mechanism research.

Results: Compared with WT mice, *SIRT1*^{+/-} mice exhibited increased adiposity and more severe insulin resistance with less thermogenesis under HFD challenge. Strikingly, *SIRT1*^{+/-} mice displayed an exacerbated brown adipose tissue (BAT) degeneration phenotype, which was characterized by lower thermogenic activity, aggravated mitochondrial dysfunction, and more mitochondrial loss. In addition, *SIRT1*^{+/-} mice showed aggravated inflammation and dysfunction in epididymal adipose tissue after HFD intervention, which also contributed to the systemic insulin resistance.

Conclusions: Diet-induced obesity and insulin resistance are associated with BAT degeneration in SIRT1-deficient mice, which further underlined the beneficial role of SIRT1 in obesity-associated metabolic disorders.

Obesity (2016) **24**, 634–642. doi:10.1002/oby.21393

Introduction

The global epidemic of obesity, which has become a major public health issue (1,2), develops with excess calories mainly storing in the white adipose tissue (WAT) when energy intake exceeds energy expenditure (3). Obesity, characterized by increased fat mass, is closely associated with insulin resistance and type 2 diabetes (4,5). A recent study has shown that obesity is associated with a brown adipose tissue (BAT) whitening phenotype that is characterized by lipid droplet accumulation and mitochondrial dysfunction and loss, which would contribute to the impaired systemic glucose metabolism (6). On the contrary, emerging evidence indicates that adipose tissue browning, including potentiating BAT function and brown remodeling of WAT, could mediate the adaptive thermogenesis and thus counteract obesity and the associated insulin resistance (7). BAT is fueled by

mitochondrial oxidation of free fatty acids (FFAs) released from triglyceride stores into the circulation and dissipates chemical energy as heat through uncoupling protein 1 (UCP1) (8). Brown remodeling of WAT, characterized by induction of beige adipocytes, confers BAT-like features onto WAT and remodels it to possess the energy disposal capacity besides the energy storage ability (9).

Mammalian sirtuin 1 (SIRT1), the closest ortholog of yeast gene Sir2, is known as a NAD⁺-dependent protein deacetylase whose activation partially mediates the metabolic benefits of caloric restriction in mammals (10,11). Accumulating evidence indicates that genetic overexpression or pharmacological activation of SIRT1 can improve obesity and insulin resistance (12–15). Nonetheless, the exact mechanism has not been clearly defined. It has been shown that specific tissue

¹ Department of Endocrinology and Metabolism, the Third Affiliated Hospital of Sun Yat-Sen University, Guangzhou, Guangdong, China. Correspondence: Jianping Weng (wjianp@mail.sysu.edu.cn). ² Guangdong Provincial Key Laboratory of Diabetology, Guangzhou, Guangdong, China ³ Antioxidant and Gene Regulation Laboratory, Pennington Biomedical Research Center, Louisiana State University System, Baton Rouge, Louisiana, USA.

See Commentary, pg. 554.

Funding agencies: This study was funded by the Program for “973” project (2012CB517506 to JW), the NIH grants (DK068036 and DK085495 to JY), the National Natural Science Foundation of China (81300705 to FX), and the Fundamental Research Funds for the Central Universities (12ykpy41 to FX).

Disclosure: The authors declared no conflict of interest.

Author contributions: FX contributed to the study design, acquisition of data, data interpretation, and manuscript writing; XZ carried out experiments, interpreted data, and wrote manuscript; BL and HC carried out experiments; HL and MC contributed to the data analysis and revision of the manuscript; JW and JY contributed to the study design and revising and editing the manuscript.

*Fen Xu and Xiaobin Zheng contributed equally to this study.

Additional Supporting Information may be found in the online version of this article.

Received: 17 August 2015; **Accepted:** 16 October 2015; **Published online 25 February 2016.** doi:10.1002/oby.21393

overexpression of SIRT1 including BAT and WAT could increase energy expenditure and thus decrease body weight and fat content under chow diet feeding (16). In line with the role of SIRT1 in energy expenditure, a number of studies have revealed the possible regulation of SIRT1 on adipose tissue browning for the adaptive thermogenesis (17,18). Overexpression of SIRT1 could enhance insulin sensitivity by potentiating BAT function and enhancing energy expenditure in mice fed with a low-fat diet (LFD) (17). Moreover, SIRT1 gain-of-function could promote brown remodeling of WAT in chow diet-fed mice in response to cold stimuli (18). However, conversely, it remains largely unknown whether SIRT1 loss-of-function would promote the degeneration of adipose tissue thermogenesis in obesity and insulin resistance induced by a high-fat diet (HFD).

In this study, we investigated the role of SIRT1 loss-of-function in diet-induced obesity and insulin resistance and the mechanism involved in adipose tissue thermogenesis using a whole-body SIRT1 heterozygous knockout (*SIRT1*^{+/-}) mouse model challenged with a HFD. As a result, we found that diet-induced obesity and insulin resistance were associated with decreased thermogenesis and BAT degeneration in SIRT1-deficient mice, which were characterized by lower thermogenic activity, aggravated mitochondrial dysfunction, and more mitochondrial loss in BAT. Additionally, we observed that SIRT1 deficiency aggravated inflammation and dysfunction in the epididymal adipose tissue, which might also contribute to the exacerbated insulin resistance. Taken together, these data further support the beneficial role of SIRT1 in obesity-associated metabolic disorders.

Methods

Animal study

SIRT1^{+/-} mice in C57BL/6J gene background were described elsewhere (19). Male *SIRT1*^{+/-} mice and their wild-type (WT) littermates were used in this study. Obesity and the associated insulin resistance were induced by feeding mice a HFD (36% fat wt/wt, D12331; Research Diets, New Brunswick, NJ) at the age of 12 weeks, while mice on a chow diet were used as lean controls (20). The mice were housed at 23 ± 1°C with a 12-h light, 12-h dark cycle and provided with ad libitum water and food. Body weight was weighed every 2 weeks and daily food intake was monitored during the diet intervention. After 16 weeks of diet intervention, mice were sacrificed under anesthesia after a 6-h fast and then plasma and tissue were harvested. All procedures were carried out in accordance with National Institutes of Health guidelines and approved by the Institute Animal Care and Use Committee (IACUC) at the Pennington Biomedical Research Center and the Animal Ethics Committees of the Sun Yat-Sen University, respectively.

Metabolic parameter measurements

Fasting plasma levels of glucose and insulin were measured with Optium Xceed glucometer (Abbott Diabetes Care) and with Mouse Serum Adipokine Multiplex Kit (MADPK-71K; LINCO Research, Billerica, MA), respectively. The homeostasis model assessment of insulin resistance (HOMA-IR) was calculated. For the glucose tolerance test (GTT), mice were fasted overnight and then injected intraperitoneally with glucose (1.5 g/kg body weight), and tail vein blood glucose levels were measured at 0, 30, 60, and 120 min. For the insulin tolerance test (ITT), mice were injected intraperitoneally with insulin (0.65 U/kg body weight, Novolin R, Novo Nordisk)

after a 6-h fast and blood glucose levels were measured as described above.

Body composition

Body composition was measured on conscious, immobilized mice using quantitative magnetic resonance EchoMRITM-100 (EchoMRI LLC, Houston, TX). Fat mass and lean mass were recorded simultaneously. Fat content was defined as the ratio of fat mass to body weight of each mouse.

Energy metabolism

Comprehensive Laboratory Animal Monitoring System (CLAMS; Columbus Instruments, Columbus, OH) was used to examine energy expenditure and heat production for individually housed mice. After 24-h adaptation, the data of oxygen consumption (VO₂), carbon dioxide production (VCO₂), and locomotor activity were simultaneously recorded. Energy expenditure and heat production were calculated as previously described (17,21).

Acute cold tolerance test

Mice were exposed to cold temperature (4°C) with free access to food and water for 6 h. Body temperature was measured every hour using a digital rectal probe (Dongxiyi Instruments Inc., Beijing, China).

Immunohistochemistry

Fresh adipose tissue was fixed for 12–16 h at room temperature in 10% neutral buffered formalin solution (v/v, HT50-1-2, Sigma), embedded in paraffin, and sectioned at 5 μm. For immunohistochemical staining, the slides were deparaffinized, blocked, and incubated overnight at 4°C with primary antibodies, and the reaction was amplified using a VECTASTAIN Elite ABC kit (PK-6102; Vector Laboratories, Burlingame, CA) and developed by the addition of AEC chromogen substrate (AEC staining kit; Sigma-Aldrich, St. Louis, MO). Antibodies are listed in Supporting Information, Table 1.

Quantitative real-time PCR

Different adipose tissue depots collected were first kept in liquid nitrogen and then stored at -80°C. Total RNA samples were isolated using Tri-Reagent (T9424, Sigma) according to the instructions provided by the manufacturer. Reverse transcription (RT) of RNA was performed with a Transcriptor First Strand cDNA Synthesis Kit (Roche Applied Science, Switzerland). Real-time PCR was performed on the LightCycler® 480 System with LightCycler® 480 SYBR Green I Master (Roche Applied Science, Switzerland). Fold change of mRNA expression was determined using the 2^{-ΔΔCT} method, with all genes normalized to the mouse β-actin. Primer sequence is available upon request.

Mitochondrial DNA content determination

Genomic DNA (gDNA) was isolated from brown fat tissue using DNeasy Blood & Tissue Kit (Qiagen). Relative mitochondrial DNA (mtDNA) content was determined by quantitative real-time PCR with primers specific for mtDNA-encoded gene (COX2) and nuclear-encoded gene (18S rRNA). The expression level ratio of COX2 to 18S

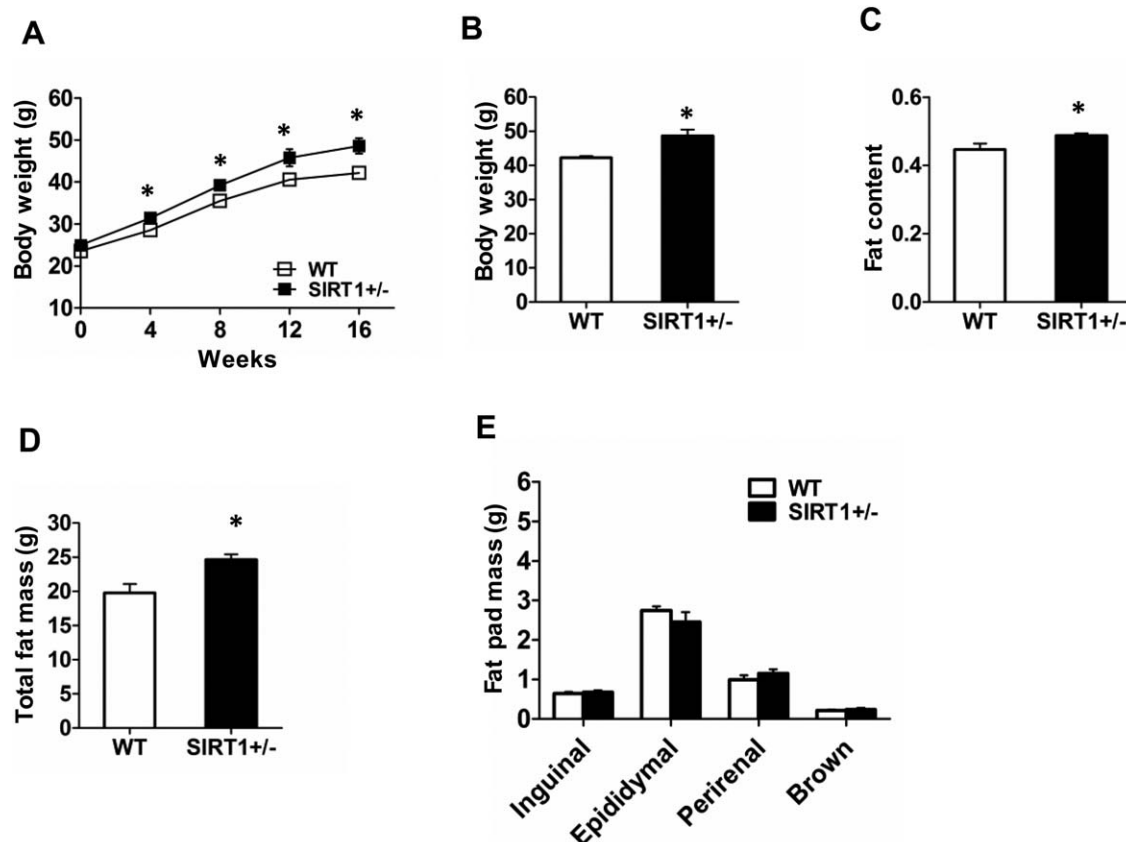


Figure 1 SIRT1 deficiency increases adiposity in mice challenged with high-fat diet (HFD). Wild-type (WT) and *SIRT1*^{+/-} mice were challenged with HFD for 16 weeks to induce obesity ($n = 6$ per group). (A) Body weight (BW) gain over time. (B) The BW on 16 weeks of HFD. (C) Fat content and (D) total fat mass determined by quantitative magnetic resonance. (E) Fat pad mass of inguinal fat, epididymal fat, perirenal fat, and brown fat. For C-E, all were determined at the end of the HFD intervention. Data are presented as mean \pm SEM. * $P < 0.05$ versus WT mice.

rRNA reflected the relative mtDNA content. Primer sequence is available upon request.

Western blotting

Different adipose tissue depots were collected and kept in liquid nitrogen, then stored at -80°C until analysis. Frozen tissues were homogenized in the whole cell lysis buffer with protease inhibitor and phosphatase inhibitor. Equal amounts of protein were separated on SDS-PAGE and blotted onto polyvinylidene fluoride membrane (Millipore, Billerica, MA). After blocking with 5% bovine serum albumin in Tris-buffered saline for 1 h at room temperature, membranes were incubated overnight at 4°C with primary antibodies. Antibodies are listed in Supporting Information, Table 1. Then the membranes were incubated with secondary antibodies (1:10000, LI-COR IRDye 800CW) at room temperature for 1 h and imaged with the Odyssey Infrared Imaging System (LI-COR Biosciences). Band intensity was quantified using the Image-Pro Plus software.

Statistical analysis

Data was expressed as mean \pm SEM. Unpaired two-tailed Student's t test was used to test statistical significance. Differences

between groups were considered statistically significant if $P < 0.05$.

Results

SIRT1 deficiency increases adiposity in HFD-challenged mice

After the diet intervention, chow diet-fed *SIRT1*^{+/-} mice were comparable with WT controls in terms of body weight gain, total fat mass, and weight of different fat pads (Supporting Information, Figure S1). In contrast, *SIRT1*^{+/-} mice began to show a significant increase in body weight at the 4th week of HFD challenge when compared with WT mice, and this increase remained for the rest of the time (Figure 1A, B). Consistent with the body weight gain, significant increases in both fat content and total fat mass determined by EchoMRI were also observed in *SIRT1*^{+/-} mice after the HFD challenge (Figure 1C, D). Importantly, the lean mass was not different between genotypes (data not shown), which indicated that the body fat increase would account for the body weight gain in HFD-fed *SIRT1*^{+/-} mice. Unexpectedly, no significant difference was observed in weight of different fat pads between genotypes after the HFD intervention, including inguinal fat, epididymal fat, perirenal

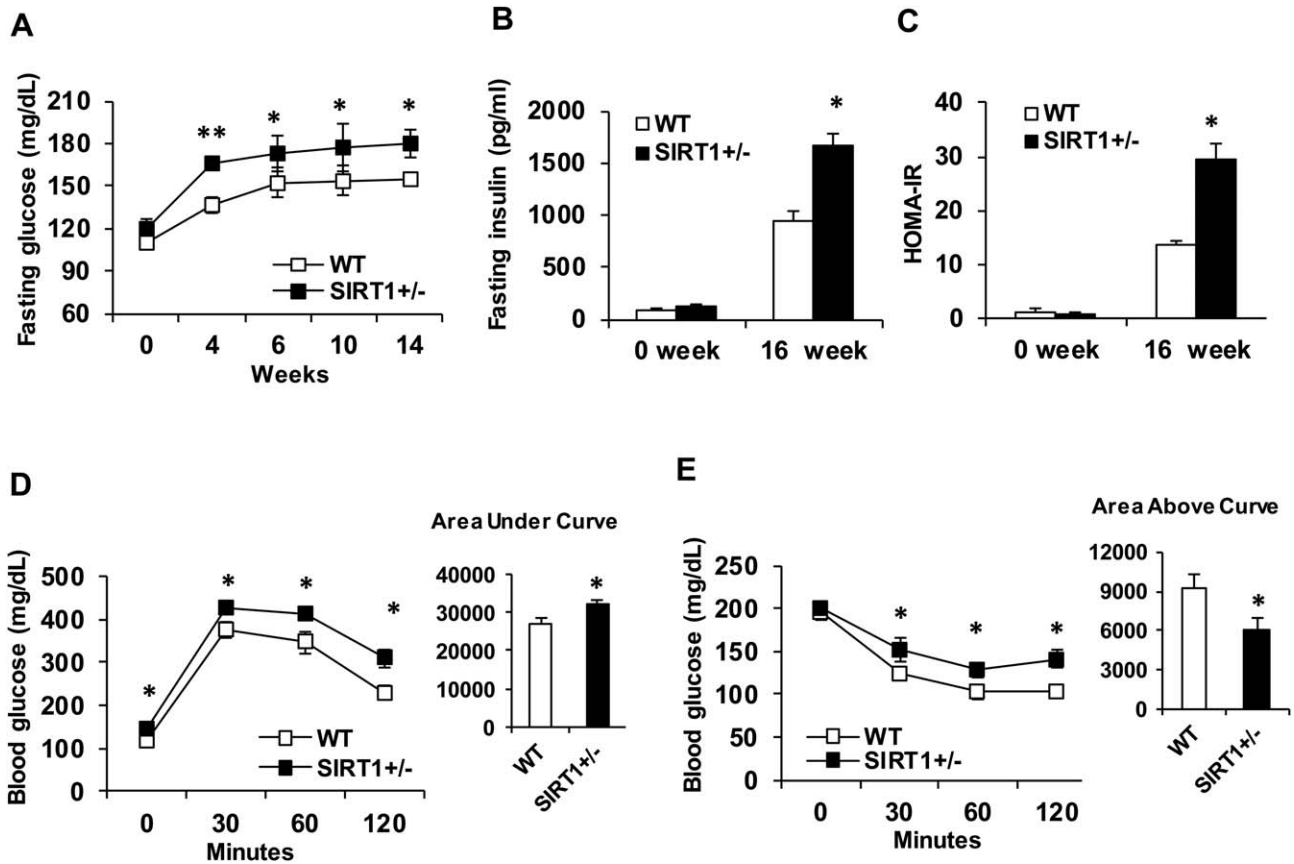


Figure 2 SIRT1 deficiency exacerbates diet-induced insulin resistance in mice challenged with high-fat diet (HFD). Wild-type (WT) and *SIRT1*^{+/-} mice were challenged with HFD for 16 weeks to induce obesity (*n* = 6 per group). (A) Fasting glucose levels in tail vein blood over time. (B) Fasting insulin levels at the beginning and the end of HFD intervention. (C) Homeostasis model assessment of insulin resistance (HOMA-IR) (D) Glucose tolerance test (GTT) and area under the curve. GTT was done at the 13th week of HFD intervention. (E) Insulin tolerance test (ITT) and area above the curve. ITT was done at the 12th week of HFD intervention. Data are presented as mean ± SEM. * *P* < 0.05 versus WT mice and ** *P* < 0.01 versus WT mice.

fat, and brown fat (Figure 1E). Nevertheless, these findings demonstrate that SIRT1 deficiency increases adiposity in HFD-challenged mice.

SIRT1 deficiency exacerbates diet-induced insulin resistance in HFD-challenged mice

To investigate the role of SIRT1 deficiency on obesity-associated insulin resistance, metabolic parameter measurements were conducted in both genotypes fed with a HFD. Compared with WT mice, *SIRT1*^{+/-} mice displayed a significantly higher fasting blood glucose level after 4 weeks of HFD challenge, which was sustained to the end of the intervention (Figure 2A). Increased fasting plasma insulin level in *SIRT1*^{+/-} mice was also observed after the HFD intervention although there was no difference at the beginning (Figure 2B). Consistently, the HOMA-IR was much higher in HFD-fed *SIRT1*^{+/-} mice (Figure 2C). GTT showed that HFD-challenged *SIRT1*^{+/-} mice had a deteriorated glucose intolerance, as indicated by the higher glucose levels at all the time points during the test and the significantly larger area under the curve (AUC) value (Figure 2D). During the ITT, higher blood glucose levels at time points 30, 60, and 120 min as well as a smaller area above the curve (AAC) value were observed in HFD-challenged *SIRT1*^{+/-} mice (Figure 2E). However, no difference

in both GTT and ITT was observed between genotypes when fed with a chow diet, which indicated that SIRT1 deficiency had no effect on insulin sensitivity in chow diet-fed mice (Supporting Information, Figure S2). Taken together, these data show that SIRT1 deficiency exacerbates diet-induced insulin resistance in HFD-challenged mice.

Lack of SIRT1 decreases thermogenesis in HFD-challenged mice

We found that the increased adiposity in HFD-fed *SIRT1*^{+/-} mice compared with WT controls was independent on diet intake, for no alteration of food intake was observed (Figure 3A). Therefore, it was possible that the increased body weight and fat content were attributable to the decreased energy expenditure in HFD-challenged *SIRT1*^{+/-} mice. As expected, *SIRT1*^{+/-} mice showed markedly decreased energy expenditure and oxygen consumption compared with WT mice after the HFD intervention during the CLAMS analysis (Figure 3B, C). Importantly, HFD-fed *SIRT1*^{+/-} mice displayed a significant decrease in heat production despite of the less locomotor activity (Figure 3D, E), confirming that the decreased energy expenditure was not only linked to physical activity, but also due to intrinsic changes in metabolism. Furthermore, acute cold tolerance test showed that HFD-fed *SIRT1*^{+/-} mice had lower body temperature than WT mice during the cold

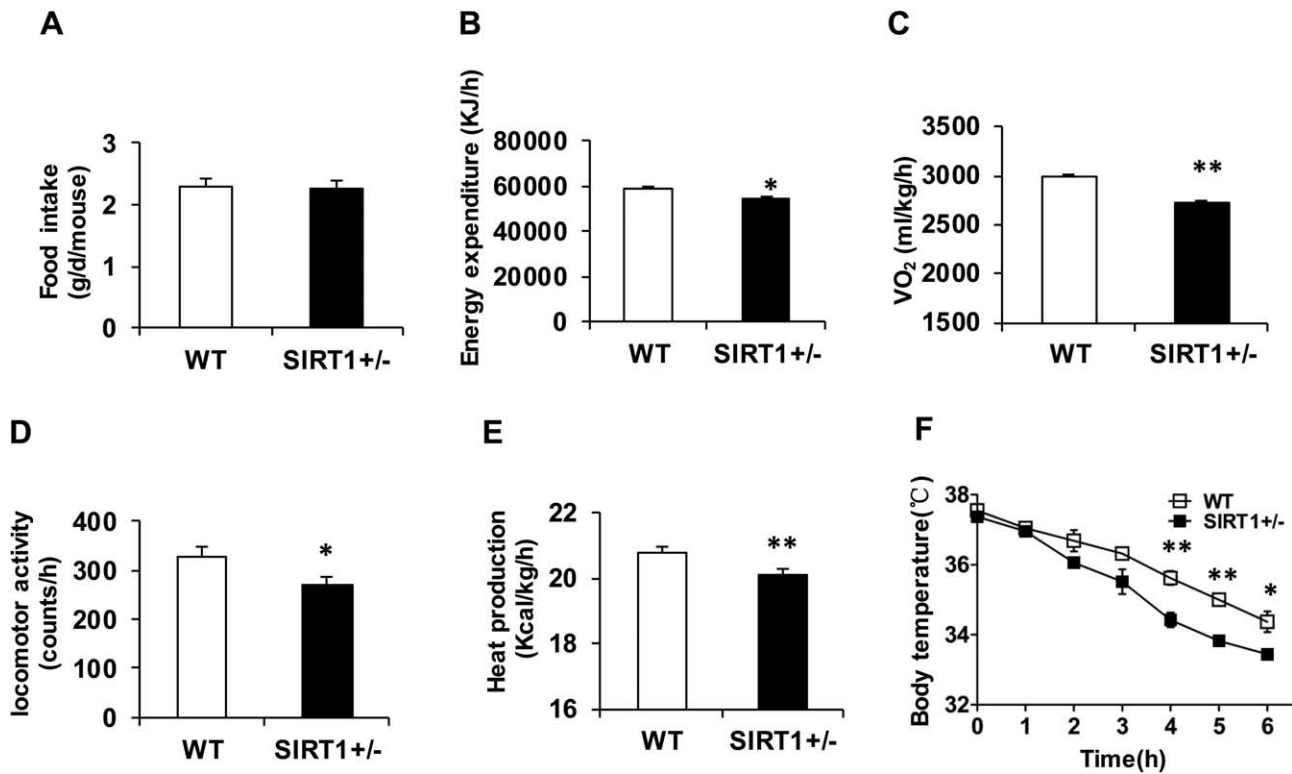


Figure 3 Lack of SIRT1 decreases thermogenesis in mice challenged with high-fat diet (HFD). Wild-type (WT) and *SIRT1*^{+/-} mice were challenged with HFD for 16 weeks to induce obesity ($n = 6$ per group). (A) Food intake was monitored daily for 3 days and average daily food intake (g) was calculated. (B) Energy expenditure. (C) Oxygen consumption (D) Locomotor activity. (E) Heat production. In panels B-E, all were determined by the metabolic cage studies. (F) Acute cold tolerance test done at the end of HFD intervention. Data are presented as mean \pm SEM. * $P < 0.05$ versus WT mice and ** $P < 0.01$ versus WT mice.

challenge (Figure 3F), further suggesting HFD-fed *SIRT1*^{+/-} mice were overall less thermogenic. However, no differences were observed between genotypes during the cold challenge under chow diet feeding (Supporting Information, Figure S3). Thus, these data demonstrate that lack of SIRT1 decreases thermogenesis in HFD-challenged mice.

SIRT1 deficiency promotes BAT degeneration in HFD-challenged mice

As BAT and the browning inguinal WAT (iWAT) are the main sites for thermogenesis in mice (7), further mechanism analysis was carried out in these tissues to account for the decreased thermogenesis in HFD-fed *SIRT1*^{+/-} mice. Not surprisingly, immunohistological staining revealed that HFD-fed *SIRT1*^{+/-} mice displayed larger lipid droplets and less expression of UCP1 in BAT (Figure 4A), suggesting a lower thermogenic activity. Both the mRNA and protein levels of thermogenic markers including UCP1 and peroxisome proliferator-activated receptor γ coactivator 1 α (PGC1 α) were significantly reduced in BAT of HFD-fed *SIRT1*^{+/-} mice (Figure 4B–D). In line with this, we also confirmed that oxidation genes were strongly downregulated in BAT of *SIRT1*^{+/-} mice, including peroxisome proliferator-activated receptor α (PPAR α), peroxisomal acyl-coenzyme A oxidase (ACOX) and carnitine palmitoyltransferase 1 β (CPT1 β) (Figure 4E). These results indicated an aggravated mitochondria dysfunction in BAT of HFD-fed *SIRT1*^{+/-} mice. Furthermore, a significant reduction of mitochondria DNA content was observed in BAT of HFD-fed *SIRT1*^{+/-} mice (Figure 4F). A similar decrease in protein levels of respiratory

complexes subunits were also seen in BAT of these mice (Figure 4G, H), indicating a more mitochondria loss. However, no significant differences in expression levels of thermogenic and oxidation genes were seen in iWAT between genotypes despite of a slight decrease in HFD-fed *SIRT1*^{+/-} mice (Supporting Information, Figure S4). Altogether, these results indicate that SIRT1 deficiency promotes BAT degeneration in HFD-challenged mice.

Lack of SIRT1 aggravates the inflammation and dysfunction in epididymal fat of HFD-induced obese mice

It is generally believed that obesity-induced chronic inflammation characterized by macrophage infiltration and inflammatory cytokine expression, especially in adipose tissue, may contribute to the development of systemic insulin resistance (22–25). Immunohistological staining revealed that protein levels of inflammatory markers in epididymal WAT (eWAT), including F4/80 and monocyte chemoattractant protein-1 (MCP-1), were significantly increased in HFD-challenged *SIRT1*^{+/-} mice compared with WT controls (Figure 5A). Additionally, HFD-fed *SIRT1*^{+/-} mice displayed a significant increase in mRNA expressions of proinflammatory cytokines including F4/80, tumor necrosis factor- α (TNF- α), MCP-1 and interleukin-1 β (IL-1 β) (Figure 5B). Classically, inflammation is considered to impair the insulin signaling and negatively influence adipose tissue function, which then contribute to the systemic

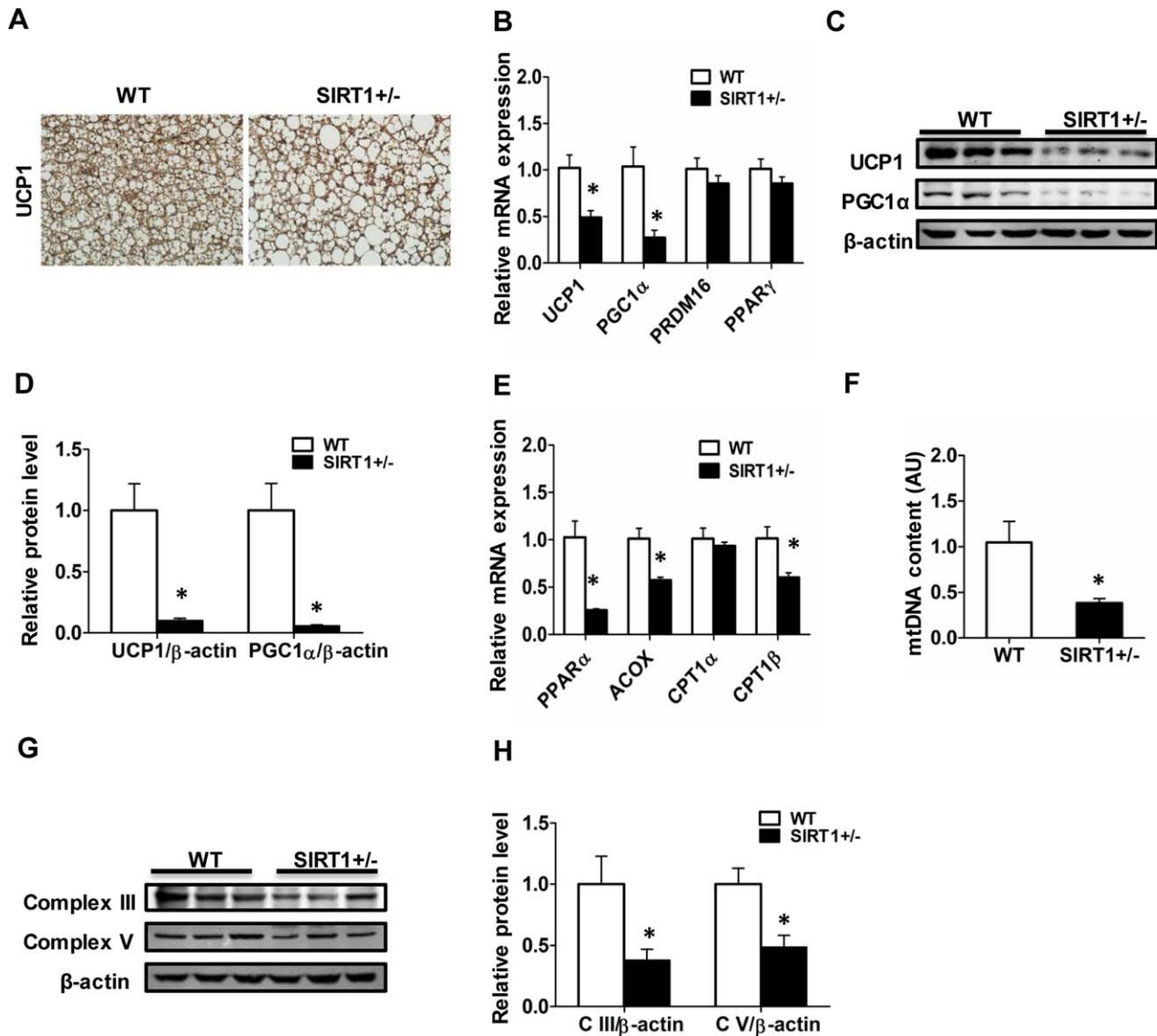


Figure 4 SIRT1 deficiency promotes brown adipose tissue (BAT) degeneration in mice challenged with high-fat diet (HFD). Wild-type (WT) and *SIRT1*^{+/-} mice were challenged with HFD for 16 weeks to induce obesity (*n* = 6 per group). (A) Representative images of uncoupling protein 1 (UCP1) immunohistochemical staining of BAT. Pictures were taken under a microscope with a $\times 40$ objective. (B) Relative mRNA expression of thermogenic genes in BAT. (C) Protein levels of UCP1 and peroxisome proliferator-activated receptor γ coactivator 1 α (PGC1 α) in BAT. (D) Densitometric quantitation of UCP1/ β -actin ratio and PGC1 α / β -actin ratio. (E) Relative mRNA expression of oxidation genes in BAT. (F) Relative mitochondrial DNA (mtDNA) content in BAT. (G) Protein analysis of mitochondrial markers in total homogenates of BAT. (H) Densitometric quantitation of mitochondrial markers. Data are presented as mean \pm SEM. * *P* < 0.05 versus WT mice. [Color figure can be viewed in the online issue, which is available at wileyonlinelibrary.com.]

insulin resistance (26,27). The reduced SIRT1 expression in eWAT of HFD-fed *SIRT1*^{+/-} mice compared with WT controls was confirmed at the protein level (Figure 5C, D). Notably, HFD-challenged *SIRT1*^{+/-} mice displayed more severely impaired insulin signaling than WT mice, as indicated by the decreased protein expression of phosphoinositide 3-kinase (p^{110 α} PI3K) and phosphorylated protein kinase B (Ser⁴⁷³p-AKT) without alteration of total AKT (Figure 5E, F). Furthermore, quantitative real-time PCR analysis confirmed a significant decrease of adiponectin mRNA expression in HFD-fed *SIRT1*^{+/-} mice despite of no change in leptin mRNA expression, suggesting a reduced adipokine secretion function of eWAT in these mice (Figure 5G, H). In this regard, these

results demonstrate that lack of SIRT1 aggravates the inflammation and dysfunction in epididymal fat of HFD-induced obese mice, which may also contribute to the exacerbated diet-induced insulin resistance aforementioned.

Discussion

SIRT1, the most conserved mammalian sirtuin, has been linked to diverse metabolic benefits in mammals. Using a whole-body *SIRT1*^{+/-} mouse model challenged with a HFD, the current study

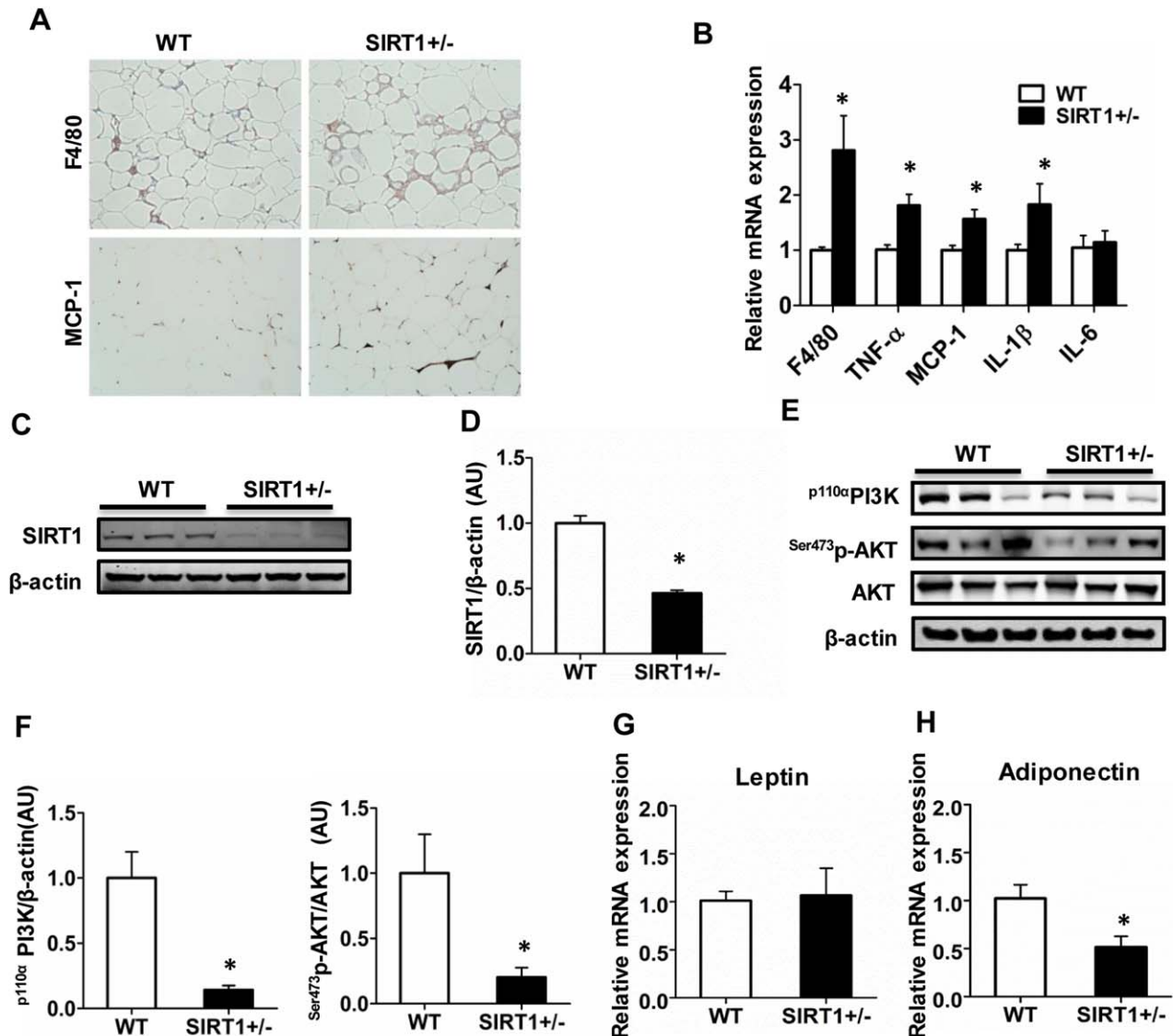


Figure 5 Lack of SIRT1 aggravates the inflammation and dysfunction in epididymal fat of high-fat diet (HFD)-induced obese mice. Wild-type (WT) and *SIRT1*^{+/-} mice were challenged with HFD for 16 weeks to induce obesity ($n = 6$ per group). (A) Representative images of F4/80 and monocyte chemoattractant protein-1 (MCP-1) immunohistochemical staining of epididymal white adipose tissue (eWAT). Pictures were taken under a microscope with a $\times 20$ objective. (B) Relative mRNA expression of key proinflammatory genes in eWAT. (C) Protein expression level of SIRT1 in eWAT. (D) Densitometric quantitation of SIRT1/ β -actin ratio. (E) Protein expression levels of the phosphoinositide 3-kinase (PI3K)/protein kinase B (AKT) pathway in eWAT. (F) Densitometric quantitation of PI3K/ β -actin ratio and p-AKT/AKT ratio. (G) Relative mRNA expression of leptin in eWAT. (H) Relative mRNA expression of adiponectin in eWAT. Data are presented as mean \pm SEM. * $P < 0.05$ versus WT mice. [Color figure can be viewed in the online issue, which is available at wileyonlinelibrary.com.]

demonstrated that diet-induced obesity and insulin resistance were associated with decreased thermogenesis and BAT degeneration in SIRT1-deficient mice, which were characterized by lower thermogenic activity, aggravated mitochondrial dysfunction, and more mitochondrial loss in BAT.

In this study, *SIRT1*^{+/-} and WT mice were fed with a HFD for 16 weeks to induce obesity and insulin resistance, while mice fed with a chow diet were used as lean controls. No differences in both adiposity and insulin sensitivity were observed between genotypes under chow diet feeding (Supporting Information, Figures S1 and

S2), which was consistent with our previous findings that *SIRT1*^{+/-} mice were normal in metabolism on the regular chow diet (19). By contrast, we found that SIRT1 deficiency increased both body weight and fat content in HFD-challenged mice (Figure 1A–C), which suggested that lack of SIRT1 exacerbated diet-induced obesity. Not surprisingly, both GTT and ITT also indicated that *SIRT1*^{+/-} mice had exacerbated glucose intolerance and insulin resistance compared with WT controls after HFD challenge (Figure 2D, E), suggesting that SIRT1 deficiency exacerbated obesity-associated insulin resistance. Our results were consistent with previous findings from other groups, which indicated that genetic

overexpression or pharmacological activation of SIRT1 could improve obesity-associated insulin resistance (12-15). In this light, our findings provide additional evidence to indicate the important role of SIRT1 in diet-induced obesity and insulin resistance.

Notably, there was no difference in food intake between genotypes (Figure 3A). As obesity develops when energy intake exceeds energy expenditure, we speculated that the increased adiposity induced by SIRT1 deficiency is due to the decreased energy expenditure. As determined by CLAMS, *SIRT1*^{+/-} mice showed remarkably reduced energy expenditure and oxygen consumption compared with WT controls after HFD challenge (Figure 3B, C), suggesting that SIRT1 deficiency decreased energy expenditure and accounted for the increased adiposity in those mice. A previous study demonstrated that SIRT1 gain-of-function decreased body weight and fat content accompanied by the increased energy expenditure under chow diet feeding using a specific tissue overexpression of SIRT1 mice model with SIRT1 knock-in into β -actin gene (16). Thus, both studies underlined the crucial role of SIRT1 in energy metabolism with loss-of and gain-of-function models, respectively.

Importantly, both heat production analysis and acute cold tolerance test showed that HFD-fed *SIRT1*^{+/-} mice were overall less thermogenic (Figure 3E, F). Intriguingly, we found an exacerbated BAT degeneration phenotype in HFD-fed *SIRT1*^{+/-} mice compared with WT controls, which might account for the decreased thermogenesis mentioned above and then contribute to the exacerbated diet-induced obesity and insulin resistance caused by SIRT1 deficiency. In our study, HFD-fed *SIRT1*^{+/-} mice displayed a lower thermogenic activity and a significant decrease in both the mRNA and protein levels of UCP1 and PGC1 α in BAT relative to WT mice, which were accompanied by the reduced mRNA levels of oxidation genes and the lower mitochondria content both at DNA and protein levels (Figure 4A-H). UCP1 is a key molecule for uncoupling respiration and dissipating chemical energy as heat (28). However, a previous study also using a whole-body *SIRT1*^{+/-} mouse model showed enhanced BAT activity as indicated by an increased UCP1 mRNA level in BAT of HFD-fed *SIRT1*^{+/-} mice compared with WT controls (29). The discrepancy between the two studies may be due to the difference in the components of the high-fat diets used. Our data were also in agreement with a recently published study of SIRT1 overexpression in mice causing an increase in UCP1 expression and BAT function when fed with a LFD (17). Of note, no significant difference was observed between genotypes in PGC1 α expression and mitochondria content in BAT of mice from the two studies mentioned above. In fact, the coactivation of AMPK signaling is crucial for the action of SIRT1 on PGC1 α activity and mitochondrial biogenesis (30). In this regard, no change in AMPK signaling was observed in the above two studies, while we found a reduced AMPK signaling in HFD-fed *SIRT1*^{+/-} mice compared with WT controls from our previous report (31), which might explain the discrepancy in the PGC1 α expression and mitochondria content of BAT from these studies. In addition, our study showed no significant difference in gene expression involved in thermogenesis and FFA oxidation in iWAT between genotypes (Supporting Information, Figure S4). By contrast, a recent study showed SIRT1 gain-of-function could promote browning remodeling of WAT in response to cold stimuli (18). These variations may be due to the lack of cold exposure in our study since prolonged cold exposure is known to induce WAT browning (32). Nevertheless, the exact mechanism for

how SIRT1 deficiency promotes BAT degeneration in HFD-challenged mice needs further investigation.

Our study also showed that SIRT1 deficiency could aggravate the inflammation in eWAT of HFD-induced obese mice (Figure 5A, B), which may contribute to the dysfunction in eWAT and the exacerbated systemic insulin resistance mentioned above. Consistently, studies from other groups also showed that myeloid-specific SIRT1 deletion increased macrophage infiltration and reduced insulin sensitivity in mice fed with a high-fat diet (33,34). Moreover, a previous study showed SIRT1 could inhibit NF- κ B transcription by deacetylating RelA/p65 subunit at lysine 310 (35). However, whether the aggravated inflammation in HFD-fed *SIRT1*^{+/-} mice in our study was secondary to the increased adiposity or induced directly by SIRT1 deficiency needed to be further studied. Furthermore, it should be emphasized that inflammation was associated with insulin resistance instead of a causal relationship, because most of the ongoing clinical trials using anti-inflammatory agents failed to generate the positive effects on the insulin resistance in patients with obesity and type 2 diabetes (26,27). The aggravated inflammation in eWAT of HFD-fed *SIRT1*^{+/-} mice may also account for the unexpected result aforementioned, which demonstrated that eWAT mass in these mice was comparable with WT controls despite a significant increase in both body weight and fat content (Figure 1). Studies have shown that inflammation could induce lipolysis and inhibit triglyceride synthesis in adipocytes, inhibiting adipocyte expansion to slow down the adipose tissue expansion (26,36). Intriguingly, we observed that HFD-fed *SIRT1*^{+/-} mice displayed more lipid accumulation in both liver and skeletal muscle than WT controls (Supporting Information, Figure S5). Taken together, we speculated that the aggravated inflammation in HFD-fed *SIRT1*^{+/-} mice may promote the lipid mobilization in eWAT and the ectopic fat accumulation in liver and skeletal muscle, which would account for the paradoxical result mentioned above.

In conclusion, our study highlights that diet-induced obesity and insulin resistance are associated with decreased thermogenesis and BAT degeneration in SIRT1-deficient mice, which provide additional evidence to underline the essential role of SIRT1 in obesity-associated metabolic disorders. **O**

© 2016 The Obesity Society

References

1. Hossain P, Kawan B, El NM. Obesity and diabetes in the developing world—a growing challenge. *N Engl J Med* 2007;356:213-215.
2. Flegal KM, Carroll MD, Ogden CL, Curtin LR. Prevalence and trends in obesity among US adults, 1999-2008. *JAMA* 2010;303:235-241.
3. Spiegelman BM, Flier JS. Obesity and the regulation of energy balance. *Cell* 2001;104:531-543.
4. Kahn SE, Hull RL, Utzschneider KM. Mechanisms linking obesity to insulin resistance and type 2 diabetes. *Nature* 2006;444:840-846.
5. Guilherme A, Virbasius JV, Puri V, Czech MP. Adipocyte dysfunctions linking obesity to insulin resistance and type 2 diabetes. *Nat Rev Mol Cell Biol* 2008;9:367-377.
6. Shimizu I, Arahamian T, Kikuchi R, et al. Vascular rarefaction mediates whitening of brown fat in obesity. *J Clin Invest* 2014;124:2099-2112.
7. Bartelt A, Heeren J. Adipose tissue browning and metabolic health. *Nat Rev Endocrinol* 2014;10:24-36.
8. Ravussin E, Galgani JE. The implication of brown adipose tissue for humans. *Annu Rev Nutr* 2011;31:33-47.
9. Wu J, Cohen P, Spiegelman BM. Adaptive thermogenesis in adipocytes: is beige the new brown? *Genes Dev* 2013;27:234-250.
10. Boily G, Seifert EL, Bevilacqua L, et al. Sirt1 regulates energy metabolism and response to caloric restriction in mice. *PLoS One* 2008;3:e1759

11. Mercken EM, Hu J, Krzysik-Walker S, et al. SIRT1 but not its increased expression is essential for lifespan extension in caloric-restricted mice. *Aging Cell* 2014;13:193-196.
12. Banks AS, Kon N, Knight C, et al. SirT1 gain of function increases energy efficiency and prevents diabetes in mice. *Cell Metab* 2008;8:333-341.
13. Pfluger PT, Herranz D, Velasco-Miguel S, Serrano M, Tschop MH. Sirt1 protects against high-fat diet-induced metabolic damage. *Proc Natl Acad Sci USA* 2008;105:9793-9798.
14. Lagouge M, Argmann C, Gerhart-Hines Z, et al. Resveratrol improves mitochondrial function and protects against metabolic disease by activating SIRT1 and PGC-1alpha. *Cell* 2006;127:1109-1122.
15. Milne JC, Lambert PD, Schenk S, et al. Small molecule activators of SIRT1 as therapeutics for the treatment of type 2 diabetes. *Nature* 2007;450:712-716.
16. Bordone L, Cohen D, Robinson A, et al. SIRT1 transgenic mice show phenotypes resembling calorie restriction. *Aging Cell* 2007;6:759-767.
17. Boutant M, Joffraud M, Kulkarni SS, et al. SIRT1 enhances glucose tolerance by potentiating brown adipose tissue function. *Mol Metab* 2015;4:118-131.
18. Qiang L, Wang L, Kon N, et al. Brown remodeling of white adipose tissue by SirT1-dependent deacetylation of Ppargamma. *Cell* 2012;150:620-632.
19. Xu F, Gao Z, Zhang J, et al. Lack of SIRT1 (Mammalian Sirtuin 1) activity leads to liver steatosis in the SIRT1 +/- mice: a role of lipid mobilization and inflammation. *Endocrinology* 2010;151:2504-2514.
20. Petro AE, Cotter J, Cooper DA, Peters JC, Surwit SJ, Surwit RS. Fat, carbohydrate, and calories in the development of diabetes and obesity in the C57BL/6J mouse. *Metabolism* 2004;53:454-457.
21. Zhang R, Maratos-Flier E, Flier JS. Reduced adiposity and high-fat diet-induced adipose inflammation in mice deficient for phosphodiesterase 4B. *Endocrinology* 2009;150:3076-3082.
22. Xu H, Barnes GT, Yang Q, et al. Chronic inflammation in fat plays a crucial role in the development of obesity-related insulin resistance. *J Clin Invest* 2003;112:1821-1830.
23. Lumeng CN, Saltiel AR. Inflammatory links between obesity and metabolic disease. *J Clin Invest* 2011;121:2111-2117.
24. Olefsky JM, Glass CK. Macrophages, inflammation, and insulin resistance. *Annu Rev Physiol* 2010;72:219-246.
25. Oh DY, Morinaga H, Talukdar S, Bae EJ, Olefsky JM. Increased macrophage migration into adipose tissue in obese mice. *Diabetes* 2012;61:346-354.
26. Wang H, Ye J. Regulation of energy balance by inflammation: common theme in physiology and pathology. *Rev Endocr Metab Disord* 2015;16:47-54.
27. Gustafson B, Hedjazifar S, Gogg S, Hammarstedt A, Smith U. Insulin resistance and impaired adipogenesis. *Trends Endocrinol Metab* 2015;26:193-200.
28. Krauss S, Zhang CY, Lowell BB. The mitochondrial uncoupling-protein homologues. *Nat Rev Mol Cell Biol* 2005;6:248-261.
29. Purushotham A, Xu Q, Li X. Systemic SIRT1 insufficiency results in disruption of energy homeostasis and steroid hormone metabolism upon high-fat-diet feeding. *FASEB J* 2012;26:656-667.
30. Canto C, Gerhart-Hines Z, Feige JN, et al. AMPK regulates energy expenditure by modulating NAD+ metabolism and SIRT1 activity. *Nature* 2009;458:1056-1060.
31. Xu F, Li Z, Zheng X, et al. SIRT1 mediates the effect of GLP-1 receptor agonist exenatide on ameliorating hepatic steatosis. *Diabetes* 2014;63:3637-3646.
32. Wu J, Bostrom P, Sparks LM, et al. Beige adipocytes are a distinct type of thermogenic fat cell in mouse and human. *Cell* 2012;150:366-376.
33. Schug TT, Xu Q, Gao H, et al. Myeloid deletion of SIRT1 induces inflammatory signaling in response to environmental stress. *Mol Cell Biol* 2010;30:4712-4721.
34. Ka SO, Song MY, Bae EJ, Park BH. Myeloid Sirt1 regulates macrophage infiltration and insulin sensitivity in mice fed a high-fat diet. *J Endocrinol.* 2015; 224:109-118.
35. Yeung F, Hoberg JE, Ramsey CS, et al. Modulation of NF-kappaB-dependent transcription and cell survival by the SIRT1 deacetylase. *EMBO J.* 2004;23:2369-2380.
36. Khan T, Muise ES, Iyengar P, et al. Metabolic dysregulation and adipose tissue fibrosis: role of collagen VI. *Mol Cell Biol* 2009;29:1575-1591.